PNAS
www.pnas.org

Supplementary Information Appendix for

Cryo-EM Structures of *Helicobacter pylori* Vacuolating Cytotoxin A Oligomeric Assemblies at Near-Atomic Resolution

Kaiming Zhang[1,*], Huawei Zhang[2,*], Shanshan Li[1,*], Grigore D. Pintilie[1], Tung-Chung Mou[3], Yuanzhu Gao[4], Qinfen Zhang[4], Henry van den Bedem[5], Michael F. Schmid[5], Shannon Wing Ngor Au[2,#], Wah Chiu[1,5,#]

[1]Departments of Bioengineering, and of Microbiology and Immunology, and James H. Clark Center, Stanford University, Stanford, CA 94305 USA.

[2]School of Life Sciences, Faculty of Science, The Chinese University of Hong Kong, Shatin, Hong Kong.

[3]Center for Biomolecular Structure and Dynamics, University of Montana, Missoula, MT 59812 USA.

[4]School of Life Sciences, Sun Yat-Sen University, Guangzhou 510275, China.

[5]Biosciences Division, SLAC National Accelerator Laboratory, Stanford University, Menlo Park, CA 94025 USA.

[6]Department of Bioengineering and Therapeutic Sciences, University of California, San Francisco, CA 94143.

[7]CryoEM and Bioimaging Division, SSRL, SLAC National Accelerator Laboratory, Stanford University, Menlo Park, CA 94025 USA.

[*]These authors contributed equally to this work.

[#]Correspondence: Wah Chiu (wahc@stanford.edu) or Shannon Au (shannon-au@cuhk.edu.hk).

This PDF file includes:

Figs. S1 to S8
Tables S1 to S2
Movies S1 to S3

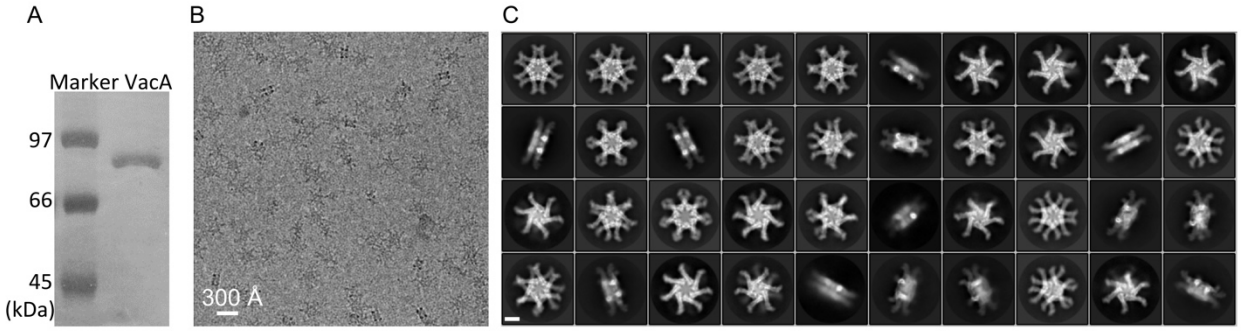

Fig. S1. Single-Particle Cryo-EM of *H. pylori* VacA. (*A*) The s1i1m1 type of VacA purified from *H. pylori* strain 60190 was examined by SDS-PAGE, with only one protein band migrating at ~88 kDa. (*B*) Representative motion corrected cryo-EM micrograph. (*C*) Reference-free 2D class averages computed in Relion. The scale bar represents 100 Å.

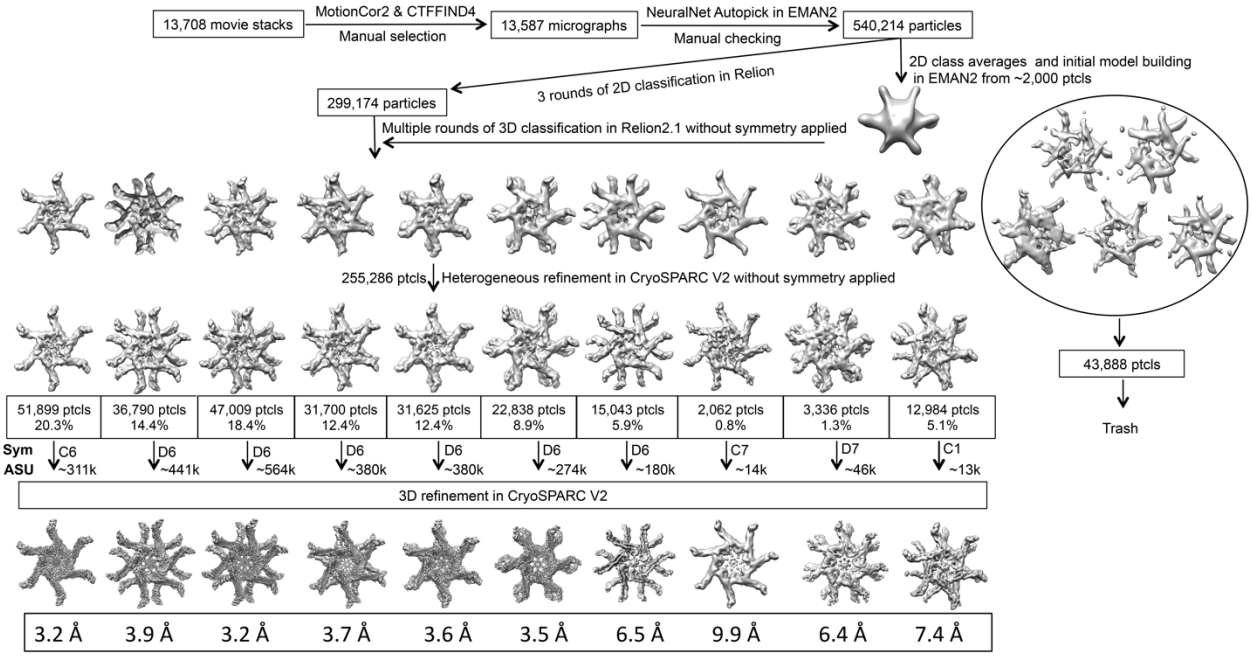

Fig. S2. Workflow of cryo-EM image processing. A total of 13,708 movie stacks were collected, motion-corrected using MotionCor2 and CTF-corrected using CTFFIND4. All particles were autopicked and then checked manually from the selected 13,587 micrographs in EMAN2. Then a total of 540,214 particle images were derived and three rounds of 2D classification were performed to remove poor 2D class averages in Relion. Meanwhile, ~ 2,000 particle images were selected to generate the 2D averages and initial model in EMAN2. Afterwards, a total of 299,174 particles were used for 3D classification in Relion without symmetry. Multiple oligomeric assemblies came out from the 3D classification, and ten selected oligomeric assemblies with their particles were used for heterogeneous and homogeneous refinement in cryoSPARC. More information can be found in the "**Materials and methods**" and **Table S1**.

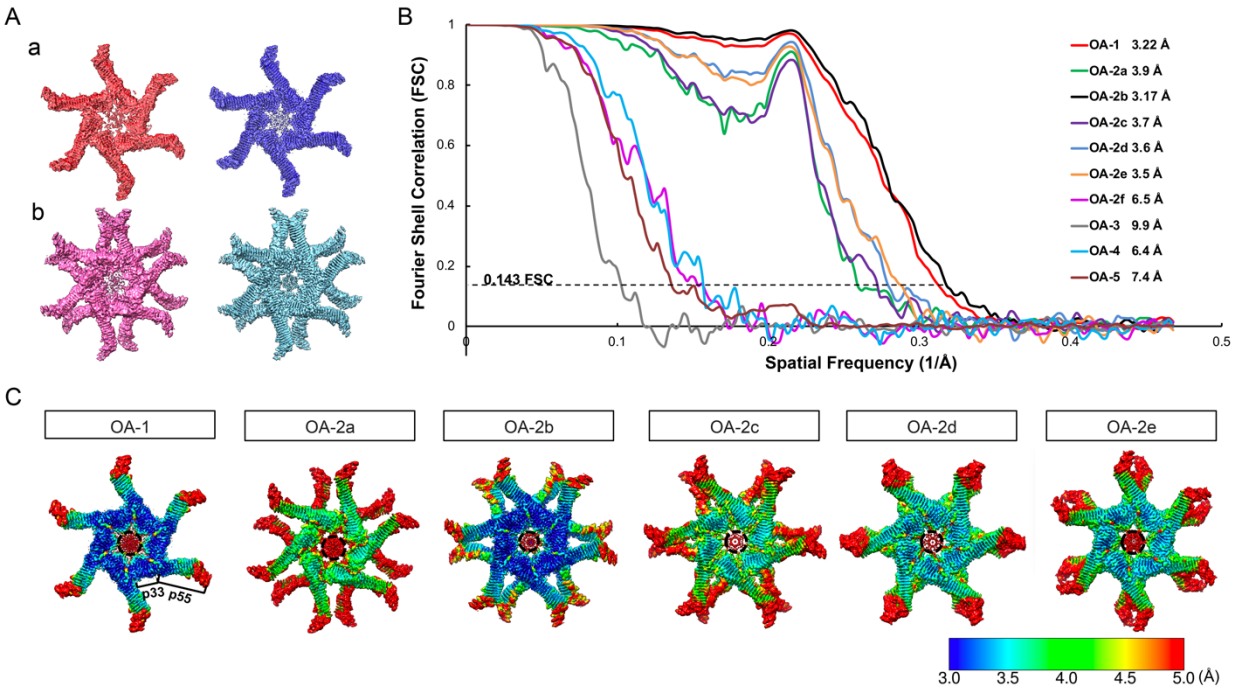

Fig. S3. 3D reconstructions of *H. pylori* VacA. (*A*) Comparison between the 3D reconstructions without and with symmetry imposed. (*a*) OA-1. Left, 3D reconstruction at 4.3 Å (red) with no symmetry imposed. Right, 3D reconstruction at 3.2 Å (blue) with C6 symmetry imposed. The cross-correlation coefficient is 0.9421. (*b*) OA-2b. Left, 3D reconstruction at 4.5 Å (pink) with no symmetry imposed. Right, 3D reconstruction at 3.2 Å (sky blue) with D6 symmetry imposed. The cross-correlation coefficient is 0.9394. (*B*) Gold standard FSC plot for the 3D reconstructions. (*C*) Resolution distribution (ResMap) for the six maps with the resolution better than 4 Å. The weak density region is shown using a dashed-line circle.

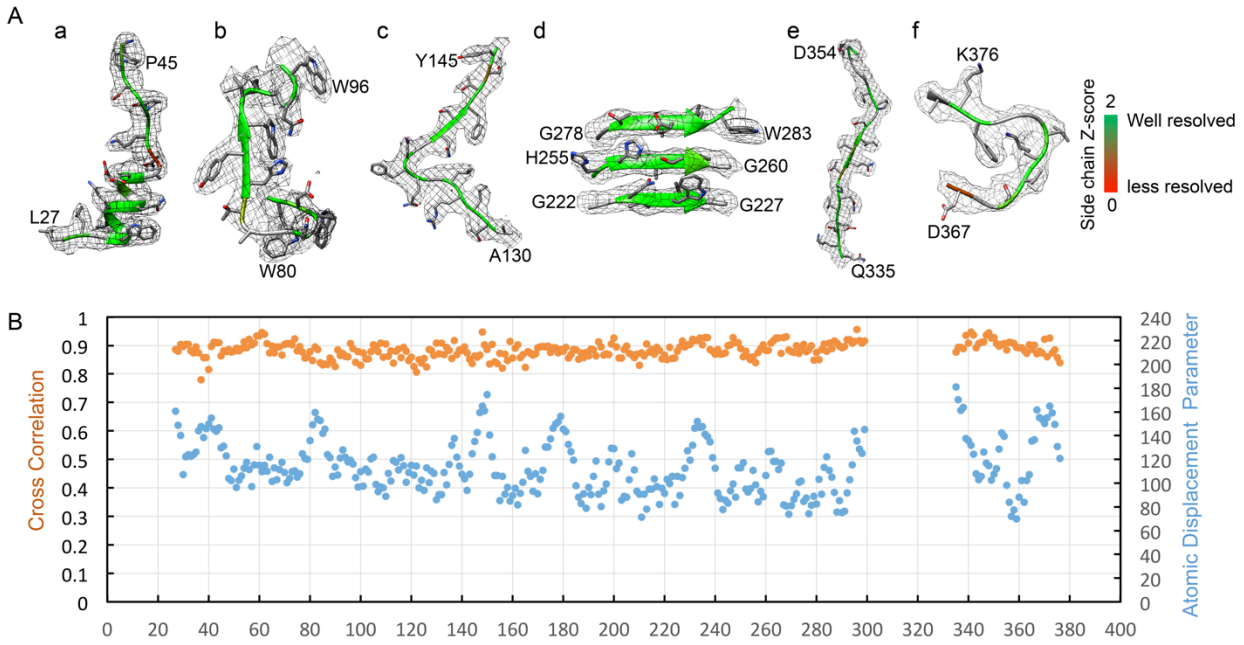

Fig. S4. Resolvability of the cryo-EM structure of VacA (OA-1). (*A*) Sample density maps of various regions of OA-1. The model backbones are shown as ribbons, with their side chain Z-scores colored on the ribbon. The higher Z-score indicating better-resolved side chains are shown in green color. Z-scores were not calculated for GLY and ALA residues (white ribbon). (*a*) The N-terminus of p33 domain (residues 27-45). (*b*) Residues 80-96 including multiple bulky side chains. (*c*) Residues 130-145 containing a loop. (*d*) A portion of the β-helix containing three β strands. (*e*) Residues 335-354. (*f*) Residues 367-376. Residues shown in (*e*) and (*f*) were not built in the p55 crystal structure (Gangwer *et al.* 2007). (*B*) Plotted scores for residues: per-residue cross-correlation coefficient between the map and model (orange dots) and per-residue atomic displacement parameter of the model (blue dots).

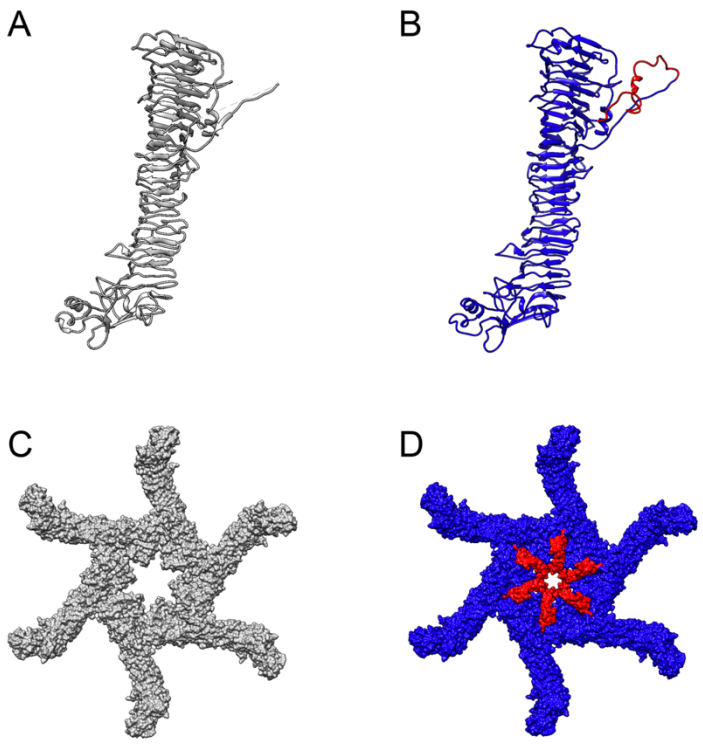

Fig. S5. The missing linker region may contribute to the central density. (*A*) The model of the VacA protomer built on the cryo-EM map (OA-1). (*B*) The model predicted by SWISS-MODEL software based on the experimental model with the missing linker region between K299 of p33 and Q335 of p55 shown in red. (*C*) Surface view of the experimental hexamer model. (*D*) Surface view of the predicted hexamer model. The missing linker region is shown in red.

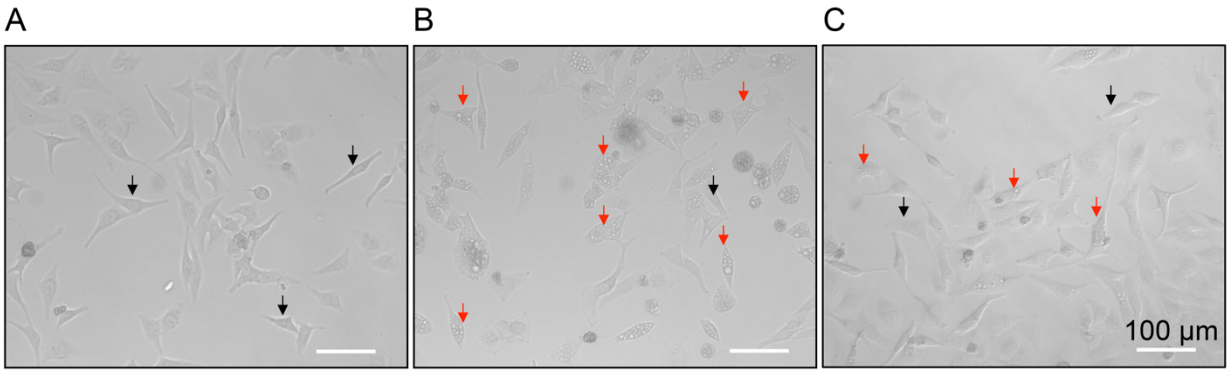

D

	Control	With acid treatment	Without acid treatment
Total cells	103	136	125
Vacuolated cells	0	127	24
Ratio of vacuolated cells	0	93%	19%

Fig. S6. Vacuolation Assay. The vacuolation activity of purified VacA with or without acid treatment was tested in *HeLa* cells. Cells without VacA addition were also included as control. *HeLa* cells were seeded and cultured on 24-well plates. VacA with or without acid treatment was then added into the cells and incubated for 3 h. Cells were then imaged under microscope. Representative images are shown in (*A*)-(*C*). Representative cells are indicated by arrows (black, healthy cells; red, vacuolated cells). *A*) Control *HeLa* cells without VacA addition. (*B*) *HeLa* cells with the addition of acid pretreated VacA. (*C*) *HeLa* cells with the addition of non-acid pretreated VacA. *D*) Number of total cells and vacuolated cells in the assay are shown.

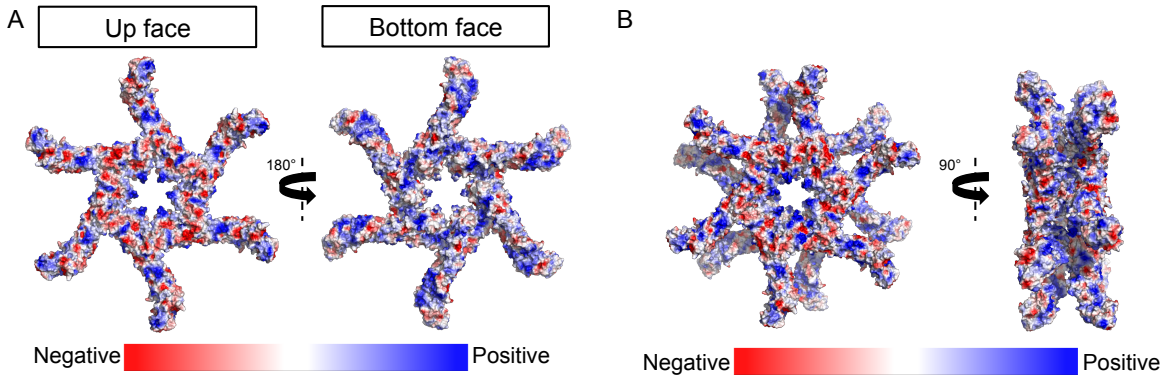

Fig. S7. Surface electrostatic potential of VacA. The surface electrostatic potential was calculated in the PyMol software using the command "generate vacuum electrostatics". (*A*) Surface electrostatic potential of the VacA hexamer (OA-1). (*B*) Surface electrostatic potential of VacA dodecamer (OA-2b).

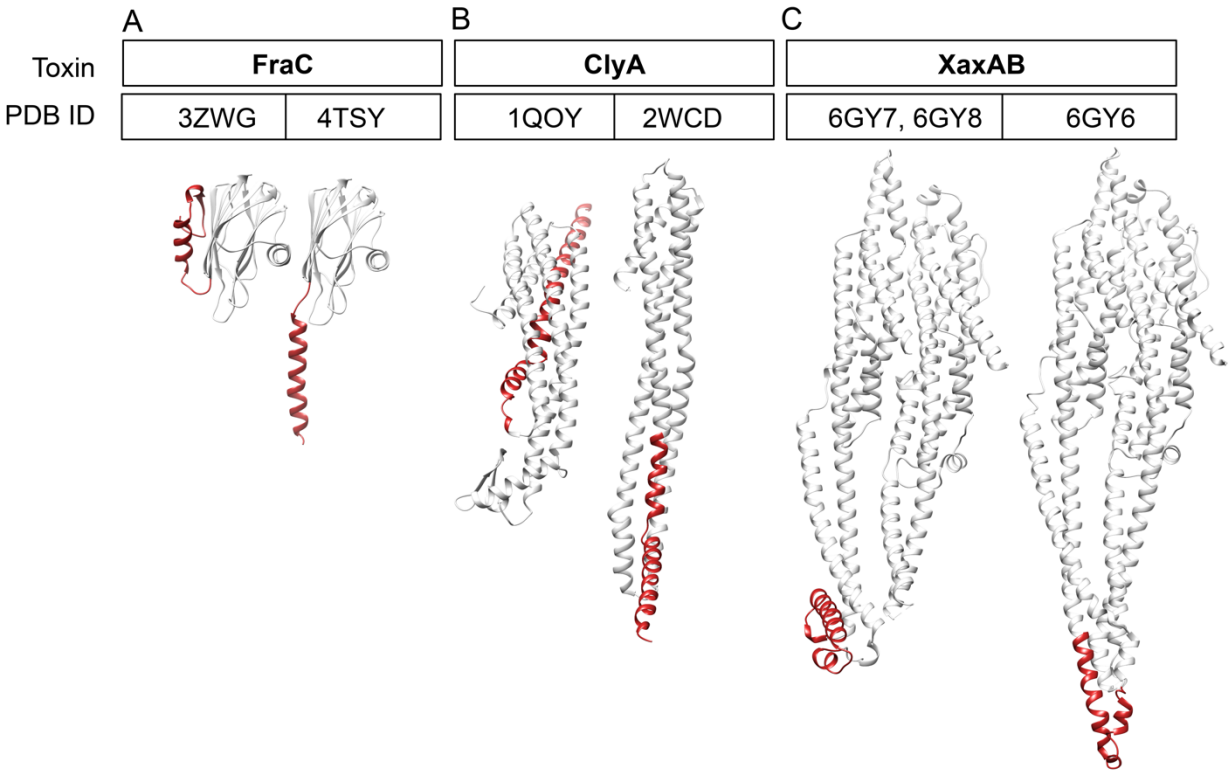

Fig. S8. Movement of α-helix during membrane insertion of toxins FraC, ClyA, and XaxAB. Similar to VacA, the membrane insertion process of other toxins like FraC, ClyA, and XaxAB also involves the movement of an amphipathic α-helix, with their other regions remaining largely unchanged. (*A*) Before (3ZWG) and after (4TSY) membrane insertion of FraC. (*B*) Before (1QOY) and after (2WCD) membrane insertion of ClyA. (*C*) Before (6GY7 and 6GY8) and after (6GY6) membrane insertion of XaxAB. XaxA (6GY8) and XaxB (6GY7) were combined together according to structural alignment with XaxAB (6GY6). Residues involved in membrane insertion are shown in red.

Table S1. Data collection and model refinement

VacA										
Data collection and processing										
Microscope	Titan Krios									
Voltage (kV)	300									
Camera	Gatan K2 Summit									
Pixel size (Å)	1.06									
Total Dose (e^- /Å^2)	42									
Defocus range (μm)	-0.7 to -2.7									
Number of micrographs	13,587									
Number of initial particles	540,214									
3D classification	OA-1	OA-2a	OA-2b	OA-2c	OA-2d	OA-2e	OA-2f	OA-3	OA-4	OA-5
Number of final particles	51,899	36,790	47,009	31,700	31,625	22,838	15,043	2,062	3,336	12,984
Symmetry	C6	D6	D6	D6	D6	D6	D6	C7	D7	C1
Resolution (0.143 FSC, Å)	3.2	3.9	3.2	3.7	3.6	3.5	6.5	9.9	6.4	7.4
Refinement										
Initial model (PDB code)	2qv3 (partial p55); *de novo* (p33 and unresolved p55)	Rigid body fitting and refinement					Rigid body fitting			
Model composition										
Non-hydrogen atoms	34,344	68,688	68,688	68,688	68,688	68,688	68,688	40,068	80,136	74,412
Protein residues	4,500	9,000	9,000	9,000	9,000	9,000	9,000	5,250	10,500	9,750
Mean B factors (Å^2)	137.67	221	145.81	205.06	147.98	182.36	N/A			
R.m.s.d										
Bond lengths (Å)	0.0078	0.0057	0.0084	0.0081	0.0056	0.0069	N/A			
Bond angles (°)	1.27	1.25	1.31	1.35	1.22	1.27	N/A			
Validation										
MolProbity score	1.95	2.11	2.07	2.2	2.05	2.09	N/A			
Clashscore	6.09	8.72	7.27	9.91	8.1	7.32	N/A			

Poor rotamers (%)	0.32	0.16	0.54	0.97	0.32	0.97	N/A
Ramachandran plot							
Favored (%)	87.06	85.9	84.68	83.81	87.42	83.33	N/A
Allowed (%)	12.94	14.1	15.32	16.19	12.58	16.67	N/A
Disallowed (%)	0	0	0	0	0	0	N/A

Table S2. Interfacing residues between two layers from VacA dodecamers (OA-2)* in PISA

	OA-2a	**OA-2b**	**OA-2c**	**OA-2d**	**OA-2e**
Resolution (Å)	3.9	3.2	3.7	3.6	3.5
Interfacing residues					
Chain a	V232/G233/A234	W82/V232/G233	G177/V232/ G233	G83/A178/ I370/V372	I370/V372/A431/ G432
Chain f'		W82			
Chain a'	V232/G233/A234	V232/G233	G177/V232/ G233	G83/A178	
Chain b'				I370/V372	I370/V372/A431/ G432

*In OA-2b, the residues whose side chain hydrophobic interactions contribute to the stability of two stacked hexamers are shown. In other dodecamers, as the resolutions are insufficient to determine the orientation of side chain, the residues with closest Cα distances between different chains are shown. The chain a in the upper layer is taken as an representative chain to illustrate the interactions with chains in the lower layer.

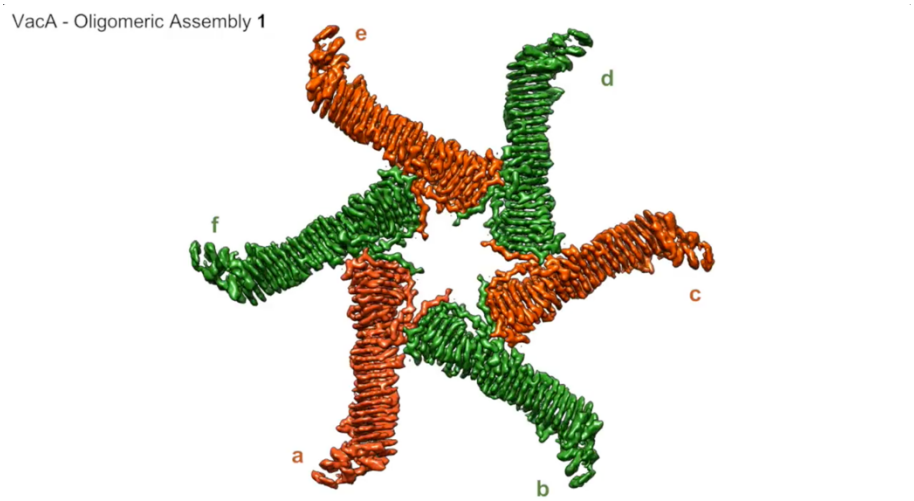

Movie S1. Movie of a 3.2-Å resolution cryo-EM map and model of VacA hexameric assembly (OA-1). Each of the 6 protomers is colored and annotated as (a,b,c,d,e, and f). The C-alpha backbone trace of a protomer made up of domain p33 and p55 are shown with the interaction residues of two adjacent protomers.

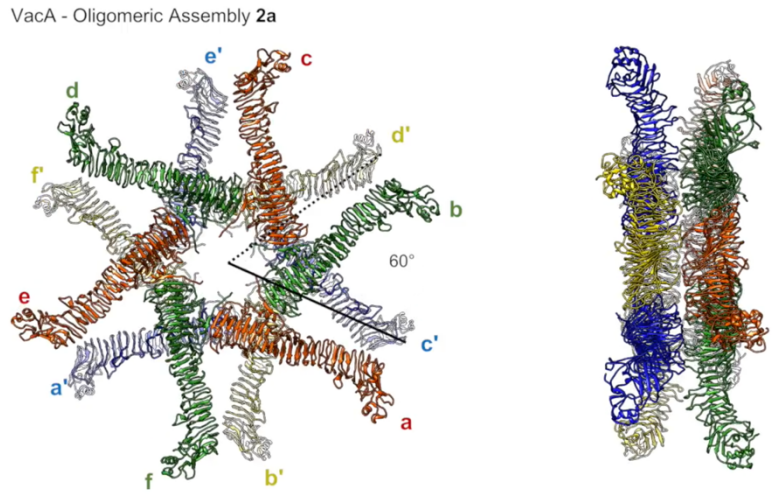

Movie S2. Movie of VacA dodecamer assemblies (OA-2a-f) conformers models. The protomer chains are annotated as a-f in one ring and a'-f" in another ring. The different kinds of hexamer-hexamer relationships are shown in the top (left) and side (right) views.

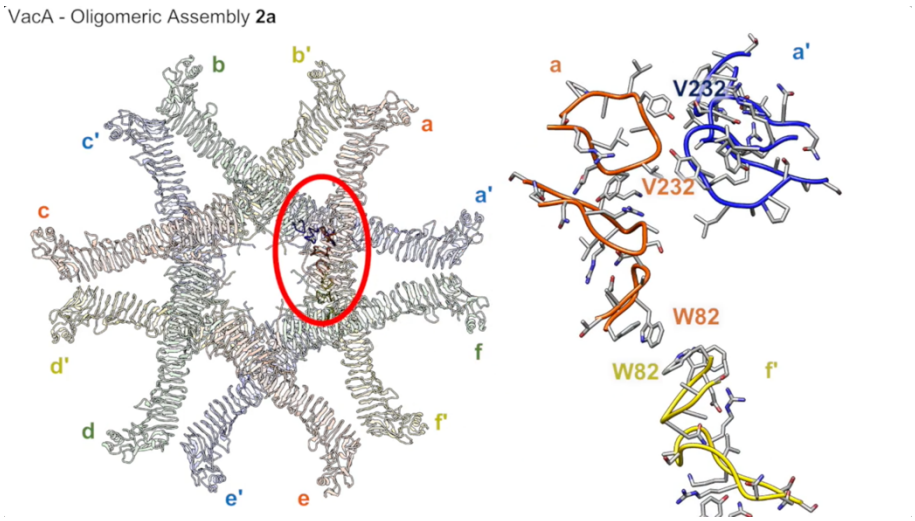

Movie S3. Movie of VacA dodecamer assemblies (OA-2a-e). Residues involved in the interface between protomers within and across two rings for five of the six dodecameric conformers determined at near-atomic resolution are shown on the right.